# Sparse grids - an approach to reduce the complexity of multiscale simulations

AERC 2018 – Sorrento – Italy

Alexander Rüttgers

German Aerospace Center (DLR)


DLR

# MODELING OF POLYMERIC FLUIDS

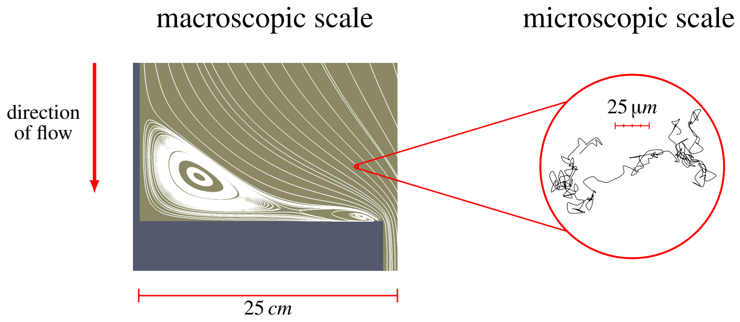


Two different modeling approaches:

| overview[1] | macroscopic | multiscale |
|---|---|---|
| cost | low | high |
| modeling accuracy | low | high |
| drawbacks | num. instabilities | |

[1] Le Bris and Lelièvre, Multiscale Model & Simul, 2009

# Microscale modeling

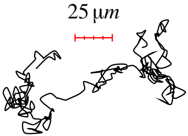


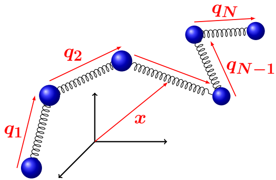


- Position vector $\boldsymbol{x}$ in flow space $\mathcal{O} \subset \mathbb{R}^3$.
- $\boldsymbol{q} = (\boldsymbol{q}_1, \ldots, \boldsymbol{q}_N)$ in configuration space $\mathcal{D} \subset \mathbb{R}^{3N}$.

# MICROSCALE MODELING

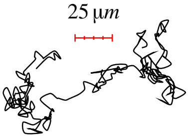


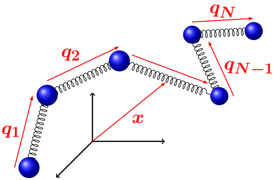


- Position vector $\boldsymbol{x}$ in flow space $\mathcal{O} \subset \mathbb{R}^3$.
- $\boldsymbol{q} = (\boldsymbol{q}_1, \ldots, \boldsymbol{q}_N)$ in configuration space $\mathcal{D} \subset \mathbb{R}^{3N}$.

Description of a polymer ensemble

- Stochastic approach:[1] random field $\boldsymbol{Q} = (\boldsymbol{Q}_1, \ldots, \boldsymbol{Q}_N)$ with $\boldsymbol{Q} : (\boldsymbol{x}, t) \in \mathcal{O} \times \mathcal{T} \mapsto \boldsymbol{Q}(\boldsymbol{x}, t)$ as $\mathcal{D}$-valued random variable.

[1] Laso and Öttinger, JNNFM, 1993

# MICROSCALE MODELING

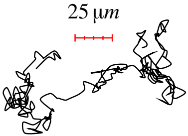


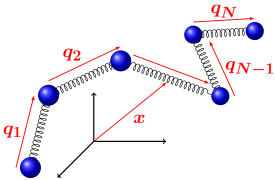


- Position vector $\boldsymbol{x}$ in flow space $\mathcal{O} \subset \mathbb{R}^3$.
- $\boldsymbol{q} = (\boldsymbol{q}_1, \dots, \boldsymbol{q}_N)$ in configuration space $\mathcal{D} \subset \mathbb{R}^{3N}$.

Description of a polymer ensemble

- Stochastic approach:[1] random field $\boldsymbol{Q} = (\boldsymbol{Q}_1, \dots, \boldsymbol{Q}_N)$ with $\boldsymbol{Q} : (\boldsymbol{x}, t) \in \mathcal{O} \times \mathcal{T} \mapsto \boldsymbol{Q}(\boldsymbol{x}, t)$ as $\mathcal{D}$-valued random variable.
- Fokker-Planck ansatz:[2] probability density function of field $\boldsymbol{Q}$
  - $\psi : (\boldsymbol{x}, \boldsymbol{q}, t) \in \mathcal{O} \times \mathcal{D} \times \mathcal{T} \subset \mathbb{R}^{3N+4} \mapsto \psi(\boldsymbol{x}, \boldsymbol{q}, t) \in \mathbb{R}^+$.
  - $\int_{\mathcal{D}} \psi(\boldsymbol{x}, \boldsymbol{q}, t)\, \mathrm{d}\boldsymbol{q} = 1$ for all $(\boldsymbol{x}, t) \in \mathcal{O} \times \mathcal{T}$.

[1] Laso and Öttinger, JNNFM, 1993 , [2] Lozinski and Chauvière, J Comp Phys, 2003

# Stochastic multiscale system

$$\frac{D\boldsymbol{U}(\boldsymbol{x},t)}{Dt} = -\nabla P(\boldsymbol{x},t) + \frac{\beta}{Re}\Delta\boldsymbol{U}(\boldsymbol{x},t) + \frac{1}{Re}\nabla\cdot\boldsymbol{\tau_p}(\boldsymbol{x},t) \tag{1}$$

$$\nabla\cdot\boldsymbol{U}(\boldsymbol{x},t) = 0 \tag{2}$$

$$\begin{aligned} d\boldsymbol{Q}(\boldsymbol{x},t) = \Big[ & -\boldsymbol{U}(\boldsymbol{x},t)\nabla\boldsymbol{Q}(\boldsymbol{x},t) + (\nabla\boldsymbol{U}(\boldsymbol{x},t))^T\boldsymbol{Q}(\boldsymbol{x},t) \\ & -\frac{1}{4\,De}\boldsymbol{A}\cdot\boldsymbol{F}(\boldsymbol{Q}(\boldsymbol{x},t))\Big]\,dt + \sigma d\boldsymbol{W}(t) \end{aligned} \tag{3}$$

$$\boldsymbol{\tau_p}(\boldsymbol{x},t) = C\sum_{i=1}^{N}\left(\mathbb{E}\left[\boldsymbol{Q}_i(\boldsymbol{x},t)\otimes\boldsymbol{F}(\boldsymbol{Q}_i(\boldsymbol{x},t))\right] - \boldsymbol{Id}\right). \tag{4}$$

for the unknown random fields $\boldsymbol{U}$, $P$, $\boldsymbol{Q}$, $\boldsymbol{\tau_p}$,
dimensionless parameters $De, Re, \beta, \sigma \in \mathbb{R}^+$
$+$ initial and boundary conditions.

(1)+(2) Navier-Stokes equations (macroscopic)
(3) Stochastic PDE (microscopic)
(4) upscaling from micro- to macroscopic scale

# 3D contraction flow

**For high Deborah number flows**

- large corner vortices occur
- streamline divergence

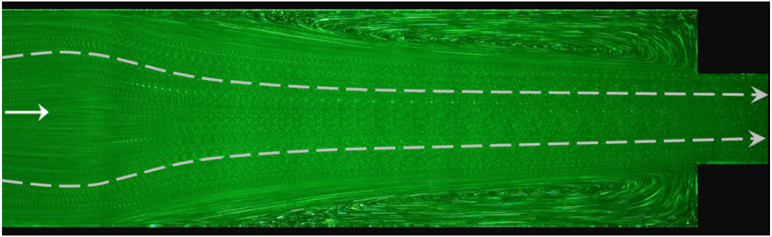

FIGURE: Visualization of contraction flow experiment[1] with $Re = 2.37, \; De = 174$

[1] Sousa, Coelho, Oliveira and Alves, JNNFM, 2011

# 3D SIMULATION RESULTS[1]

- 8 multiscale simulations.

| Simulation parameters | |
|---|---|
| Deborah number $De$ | 24.1, 108, 157 |
| spring model | FENE chain |
| spring segments $N$ | 1, 3, 5 |
| resolution $M_g$ | $380 \times 64 \times 64$ |
| samples per cell $M_s$ | 1200 |

[1] published in Griebel and R., JNNFM, 2014

# 3D SIMULATION RESULTS[1]

- 8 multiscale simulations.
- All elastic effects reproduced in simulation.
- No stability issues occurred.
- Results correspond with experimental measurements.

| **Simulation parameters** | |
|---|---|
| Deborah number $De$ | 24.1, 108, 157 |
| spring model | FENE chain |
| spring segments $N$ | 1, 3, 5 |
| resolution $M_g$ | $380 \times 64 \times 64$ |
| samples per cell $M_s$ | 1200 |

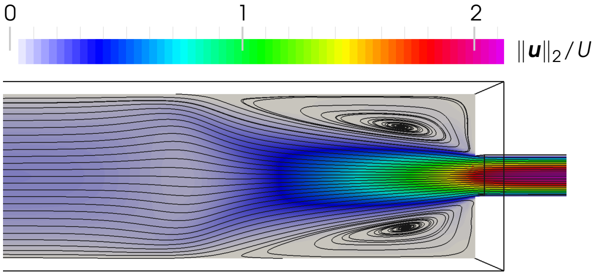


FIGURE: Simulation of 5-segment chain with $De = 157$.

[1] published in Griebel and R., JNNFM, 2014

# 3D SIMULATION RESULTS[1]

- 8 multiscale simulations.
- All elastic effects reproduced in simulation.
- No stability issues occurred.
- Results correspond with experimental measurements.

| Simulation parameters | |
|---|---|
| Deborah number $De$ | 24.1, 108, 157 |
| spring model | FENE chain |
| spring segments $N$ | 1, 3, 5 |
| resolution $M_g$ | $380 \times 64 \times 64$ |
| samples per cell $M_s$ | 1200 |

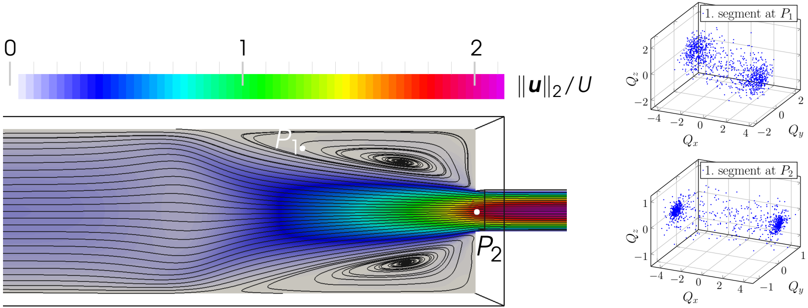


FIGURE: Simulation of 5-segment chain with $De = 157$.

[1] published in Griebel and R., JNNFM, 2014

# Complexity of multiscale simulations

- $M_g$ grid cells in space,
- $M_s$ samples per grid cell,
- spring model with $N$ segments.

# Complexity of multiscale simulations

- $M_g$ grid cells in space,
- $M_s$ samples per grid cell,
- spring model with $N$ segments.

MACROSCALE storage size of order $\mathcal{O}(M_g)$ in each time step.

MICROSCALE Complexity of discrete samples of order $\mathcal{O}(M_g \cdot M_s \cdot N)$ per time step.

# Complexity of multiscale simulations

- $M_g$ grid cells in space,
- $M_s$ samples per grid cell,
- spring model with $N$ segments.

MACROSCALE storage size of order $\mathcal{O}(M_g)$ in each time step.

MICROSCALE Complexity of discrete samples of order $\mathcal{O}(M_g \cdot M_s \cdot N)$ per time step.

| 3D contraction flow | microscale $\boldsymbol{Q}$ |
|---|---|
| spatial grid $M_g$ | $380 \times 64 \times 64$ |
| samples per cell $M_s$ | 1200 |
| spring segments $N$ | 5 |
| total samples | $1.87 \cdot 10^9$ |
| sample dimensionality | 15-dim |
| storage | 208 GB |
| comput. time (256 CPUs) | 7-8 weeks |

# Complexity of multiscale simulations

- $M_g$ grid cells in space,
- $M_s$ samples per grid cell,
- spring model with $N$ segments.

MACROSCALE storage size of order $\mathcal{O}(M_g)$ in each time step.

MICROSCALE Complexity of discrete samples of order $\mathcal{O}(M_g \cdot M_s \cdot N)$ per time step.

| 3D contraction flow | microscale $\boldsymbol{Q}$ |
|---|---|
| spatial grid $M_g$ | $380 \times 64 \times 64$ |
| samples per cell $M_s$ | 1200 |
| spring segments $N$ | 5 |
| total samples | $1.87 \cdot 10^9$ |
| sample dimensionality | 15-dim |
| storage | 208 GB |
| comput. time (256 CPUs) | 7-8 weeks |

Solution approach

1. Parallelization.
2. Model complexity reduction.

## Sparse grids and combination technique[1,2]

- Approximation of full grid solution $\boldsymbol{u_l} \in V_{\boldsymbol{l}}$ as a **combination of coarse full grid solutions** $\boldsymbol{u_m} \in V_{\boldsymbol{m}}$.
- Multi-indices $\boldsymbol{m}, \boldsymbol{l} \in \mathcal{I} \subset \mathbb{N}^d$ denote discretization accuracy.
- Approach bases on multivariate extrapolation.

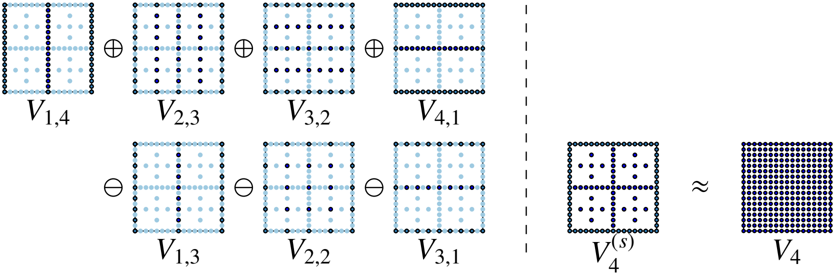


FIGURE: Classical $2d$ combination technique.

---

[1] Griebel, Schneider, Zenger, Iterative Meth Lin Alg, 1992

[2] Bungartz, Griebel, Rüde, Comput Meth Appl Mech Eng, 1994

## Sparse grids and combination technique[1,2]

- Approximation of full grid solution $\boldsymbol{u_l} \in V_{\boldsymbol{l}}$ as a **combination of coarse full grid solutions $\boldsymbol{u_m} \in V_{\boldsymbol{m}}$**.
- Multi-indices $\boldsymbol{m}, \boldsymbol{l} \in \mathcal{I} \subset \mathbb{N}^d$ denote discretization accuracy.
- Approach bases on multivariate extrapolation.
- Combination technique is intrinsically parallel.
- Existing multiscale solver can be **reused**.

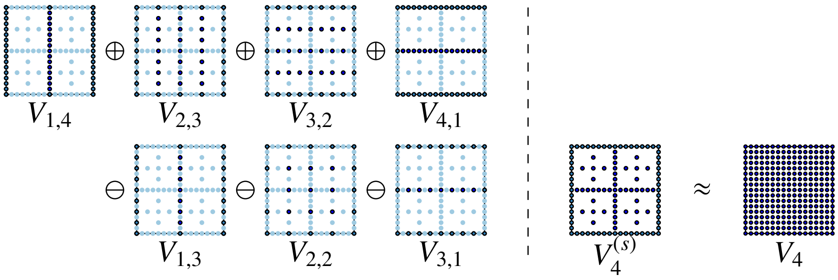


FIGURE: Classical $2d$ combination technique.

[1] Griebel, Schneider, Zenger, Iterative Meth Lin Alg, 1992
[2] Bungartz, Griebel, Rüde, Comput Meth Appl Mech Eng, 1994

# Multiscale model dimensions

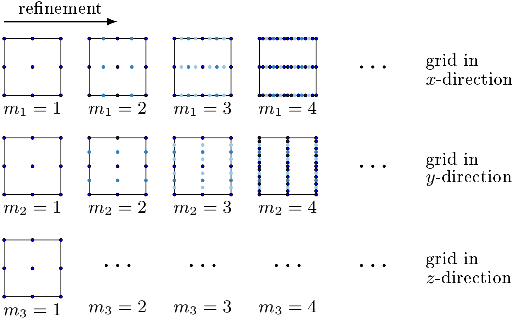


Discretization and modeling grid

# MULTISCALE MODEL DIMENSIONS

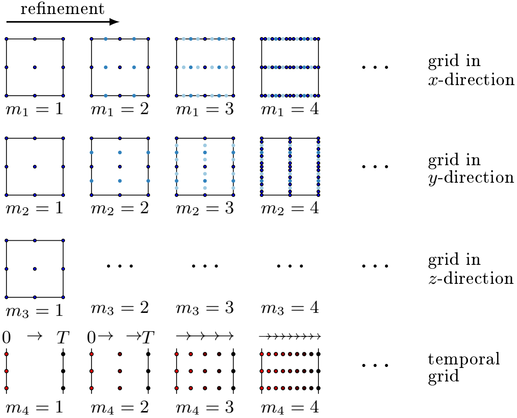


Discretization and modeling grid

# Multiscale model dimensions

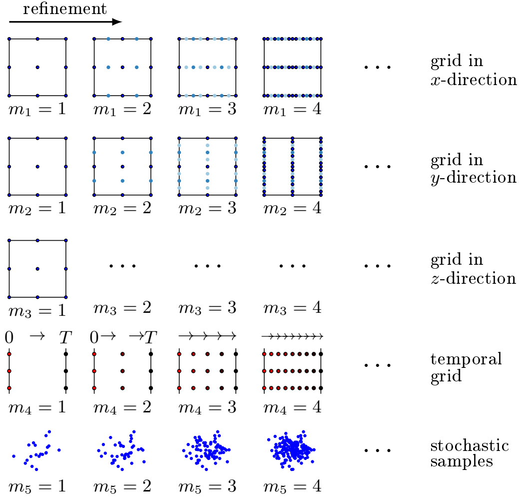


Discretization and modeling grid

# Multiscale model dimensions

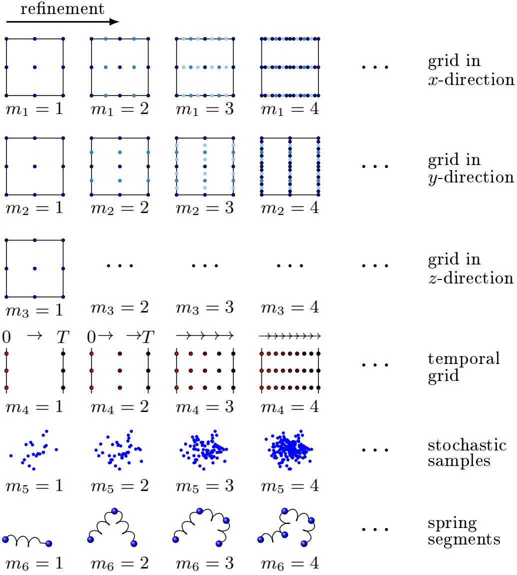


Discretization and modeling grid

## QUESTION

How can an appropriate index set $\mathcal{I}$ be generated?

## Question

How can an appropriate index set $\mathcal{I}$ be generated?

### Adaptive refinement of the $d$ dimensions[1,2]

- Start: $\mathcal{I}^{(1)} = \{1, \ldots, 1\} \in \mathbb{N}^d$.

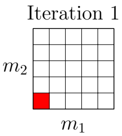


Example for $d = 2$:

Index set $\mathcal{I}^{(1)} = (1, 1)$

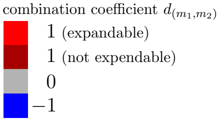


[1] Gerstner and Griebel, Numer Algorithm, 1998 [2] Gerstner and Griebel, Comput, 2003

## Question

How can an appropriate index set $\mathcal{I}$ be generated?

### Adaptive refinement of the $d$ dimensions[1,2]

- Start: $\mathcal{I}^{(1)} = \{1, \ldots, 1\} \in \mathbb{N}^d$.
- Iteration $it \to it + 1$:
  - Consider cost $c_{\boldsymbol{m}}$ and benefit $b_{\boldsymbol{m}}$ for all $\boldsymbol{m} \in \mathcal{I}^{(it)}$.
  - Refinement of the space with maximum cost-benefit ratio $g_{\boldsymbol{m}}$ in all $d$ dimensions, if permitted.

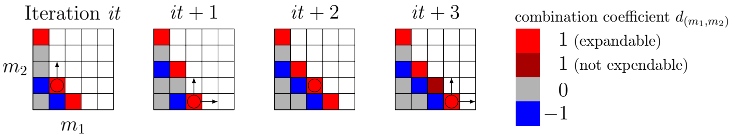


[1] Gerstner and Griebel, Numer Algorithm, 1998 [2] Gerstner and Griebel, Comput, 2003

# SIMULATION 1: COUETTE FLOW[1]

- Non-Newtonian fluid in 2D channel: velocity field $\boldsymbol{u} = (u, v)$.
- At $t = 0$ the fluid is at rest.
- Constant shearing with $\dot{\gamma} = \frac{\partial u}{\partial y} = 1$ for $t > 0$.

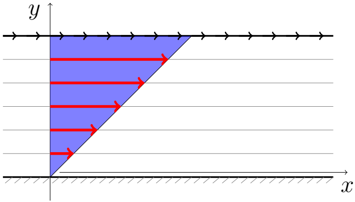


(a) shear flow ($t \to \infty$)

[1] published in R. and Griebel, Applied Mathematics and Computation, 2018

# Simulation 1: Couette flow[1]

- Non-Newtonian fluid in 2D channel: velocity field $\boldsymbol{u} = (u, v)$.
- At $t = 0$ the fluid is at rest.
- Constant shearing with $\dot{\gamma} = \frac{\partial u}{\partial y} = 1$ for $t > 0$.
- Spring model with $N = 1$ segment.
- Aim: Accurate approximation of oscillating velocity component $u$.

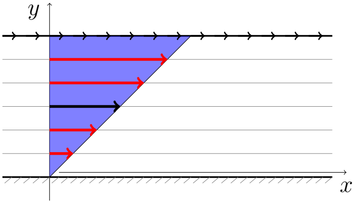


(a) shear flow ($t \to \infty$)

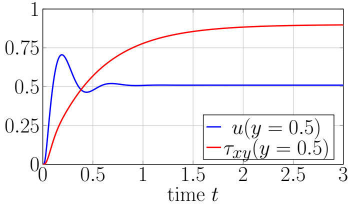


(b) Evolution at position $y = 0.5$ in channel of height 1

[1] published in R. and Griebel, Applied Mathematics and Computation, 2018

# DIMENSION-ADAPTIVE REFINEMENT

- 3 directions of refinement:
  - spatial grid
  - stochastic grid
  - temporal grid
- Initial level $(1/\Delta y_{m_1}, \text{Samples } m_2, 1/\Delta t_{m_3}) = (2, 256, 16)$.
- Refinement by a factor of 2 in each level.

# Dimension-adaptive refinement

- 3 directions of refinement:
  - spatial grid
  - stochastic grid
  - temporal grid
- Initial level $(1/\Delta y_{m_1}, \text{Samples } m_2, 1/\Delta t_{m_3}) = (2, 256, 16)$.
- Refinement by a factor of 2 in each level.
- Cost-benefit ratio index $g_{\boldsymbol{m}}$ indicates directions of refinement.

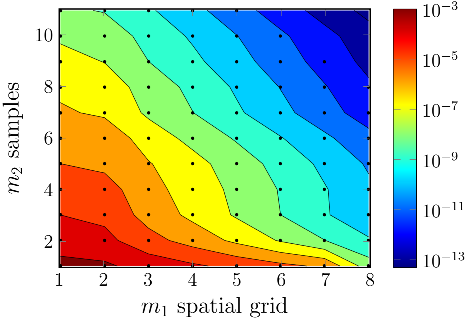


Figure: Cost-benefit index $g_{(m_1,m_2,m_3=3)}$ for $\Delta t_{m_3} = 1/64$

# Visualization of the algorithm

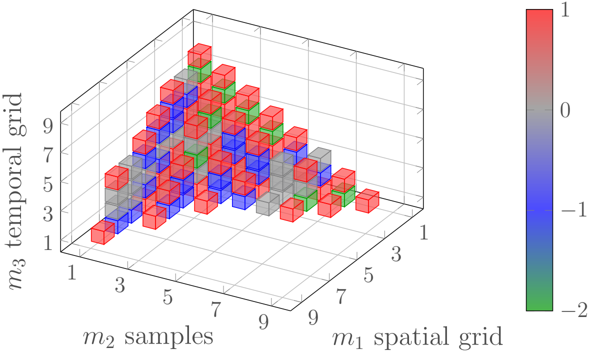


Figure: 3D index set $\mathcal{I}^{(it)}$ in iteration step $it = 90$.

# Convergence of combination technique

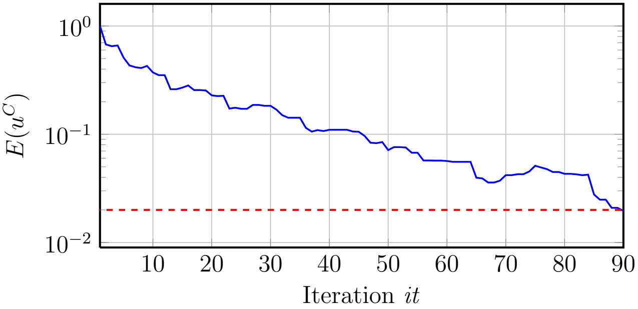


Figure: Relative error $E(u^{C,it}) = \|u^{C,it} - u_{\text{ref}}\|_2 / \|u^{C,it=1} - u_{\text{ref}}\|_2$

# CONVERGENCE OF COMBINATION TECHNIQUE

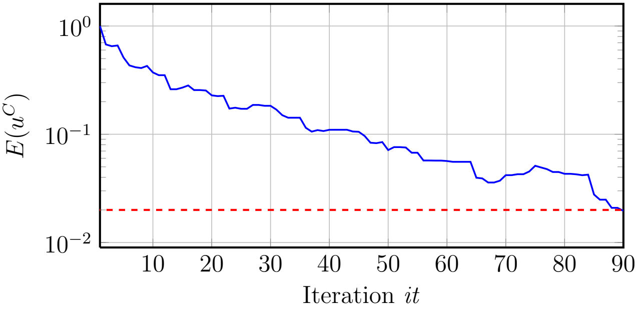


FIGURE: Relative error $E(u^{C,it}) = \|u^{C,it} - u_{\text{ref}}\|_2 / \|u^{C,it=1} - u_{\text{ref}}\|_2$

**Error and cost analysis**

- Adaptive solution $u^{C,it=90}$ has similar accuracy as $u_{7,7,7}$.
- Complexity of $u^{C,it=90}$ is $\approx$ 10-times lower than full grid $u_{7,7,7}$.

# SIMULATION 2: 3D EXTENSIONAL FLOW[1]

- Non-Newtonian fluid in steady 3D extensional flow.

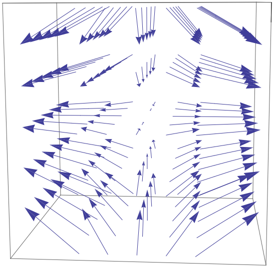

(a) extensional flow

[1] published in R. and Griebel, Applied Mathematics and Computation, 2018

# SIMULATION 2: 3D EXTENSIONAL FLOW[1]

- Non-Newtonian fluid in steady 3D extensional flow.
- Aim: Temporal evolution of stress tensor $\boldsymbol{\tau_p}$ for nonlinear FENE chain with $N = 5$ segments.
- $3N + 1$-dimensional density $\psi : (\boldsymbol{q}, t) \in \mathbb{R}^{3N} \times \mathbb{R} \mapsto \psi(\boldsymbol{q}, t) \in \mathbb{R}^+$.

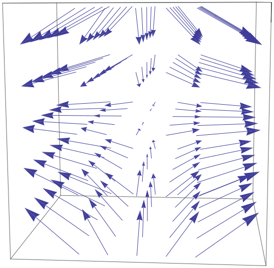

(a) extensional flow

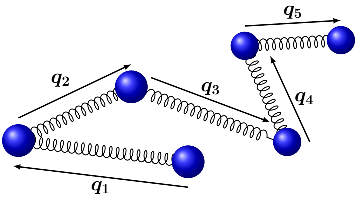


(b) 5-segment FENE chain

[1] published in R. and Griebel, Applied Mathematics and Computation, 2018

# Dimension-adaptive refinement

- 3 directions of refinement:
  - stochastic grid
  - temporal grid
  - spring model grid (modeling error)
- Balancing of numerical and modeling errors.

# Dimension-adaptive refinement

- 3 directions of refinement:
  - stochastic grid
  - temporal grid
  - spring model grid (modeling error)
- Balancing of numerical and modeling errors.
- Initial level (samples $m_1, 1/\Delta t_{m_2}$, segments $m_3$) $= (1024, 2, 1)$.
- Refinement by factor 2 in stochastic/time, +1 for spring model grid.

# Dimension-adaptive refinement

- 3 directions of refinement:
  - stochastic grid
  - temporal grid
  - spring model grid (modeling error)
- Balancing of numerical and modeling errors.
- Initial level $(\text{samples } m_1, 1/\Delta t_{m_2}, \text{segments } m_3) = (1024, 2, 1)$.
- Refinement by factor 2 in stochastic/time, +1 for spring model grid.
- Cost reduction by factor of 5 compared to a classical full grid.

# Dimension-adaptive refinement

- 3 directions of refinement:
  - stochastic grid
  - temporal grid
  - spring model grid (modeling error)
- Balancing of numerical and modeling errors.
- Initial level (samples $m_1$, $1/\Delta t_{m_2}$, segments $m_3$) $= (1024, 2, 1)$.
- Refinement by factor 2 in stochastic/time, +1 for spring model grid.
- Cost reduction by factor of 5 compared to a classical full grid.

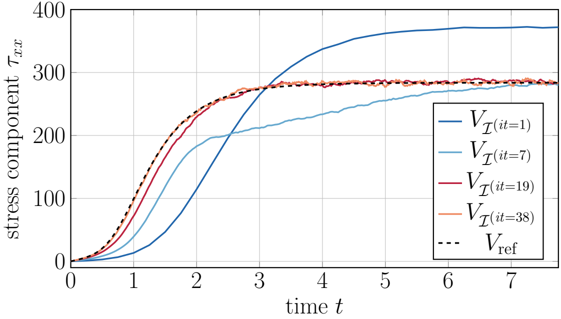


FIGURE: Comparison of approximation spaces for $\tau_{xx}$.

## Summary

1. Reduction of enormous computing time with twofold parallelism:
   - parallelization (*Atacama* cluster 1248 CPUs).
   - sparse grid combination technique.

## Summary

1. Reduction of enormous computing time with twofold parallelism:
   - parallelization (*Atacama* cluster 1248 CPUs).
   - sparse grid combination technique.
2. Application of sparse grids for non-Newtonian fluids:
   - Balancing of numerical and modeling errors.
   - Computation effort reduced by up to one order of magnitude.

## Summary

1. Reduction of enormous computing time with twofold parallelism:
   - parallelization (*Atacama* cluster 1248 CPUs).
   - sparse grid combination technique.
2. Application of sparse grids for non-Newtonian fluids:
   - Balancing of numerical and modeling errors.
   - Computation effort reduced by up to one order of magnitude.

## References


- M. Griebel, A. Rüttgers
  **Multiscale simulations of 3D viscoelastic flows in a square-square contraction**
  *J Non-Newton Fluid Mech*, 205:41-63, 2014
- A. Rüttgers, M. Griebel
  **Multiscale simulation of polymeric fluids using the sparse grid combination technique**
  *Appl Math & Comput*, 319:425-443, 2018


Thank you for your attention!

# References (1/2)


1. C. Le Bris, T. Lelièvre.
   **Multiscale modelling of complex fluids: a mathematical initiation**
   *Multiscale Modeling and Simulation in Science*, 49–137, 2009
2. M. Laso, H. Öttinger.
   **Calculation of viscoelastic flow using molecular models**
   *J Non-Newton Fluid Mech*, 47:1–20, 1993
3. A. Lozinski, C. Chauvière.
   **A fast solver for Fokker–Planck equation applied to viscoelastic flows calculations**
   *J Comp Phys*, 189:607–625, 2003
4. P. Sousa, P. Celho, M. Oliveira, M. Alves
   **Effect of the contraction ratio upon viscoelastic fluid flow in three-dimensional square–square contractions**
   *Chem Eng Sci*, 66:998–1009, 2011
5. M. Griebel, M. Schneider, C. Zenger
   **A combination technique for the solution of sparse grid problems**
   *Iterative Meth Lin Alg*, 263–281, 199

# References (2/2)


6. H. Bungartz, M. Griebel, U. Rüde
**Extrapolation, combination, and sparse grid techniques for elliptic boundary value problems**
*Comput Meth Appl Mech Eng*, 243–252, 1994

7. T. Gerstner, M. Griebel
**Numerical integration using sparse grids**
*Numer Algorithm*, 18:209-232, 1998

8. T. Gerstner, M. Griebel
**Dimension–adaptive tensor–product quadrature**
*Comput*, 71:65-87, 2003